

## Article

# Use of MD Simulation for Investigating Diffusion Behaviors between Virgin Asphalt and Recycled Asphalt Mastic

Shuqi Chen <sup>1</sup>, Qing Yang <sup>1,\*</sup>, Xin Qiu <sup>1</sup>, Ke Liu <sup>1</sup>, Shanglin Xiao <sup>1</sup> and Wenyi Xu <sup>2</sup>

<sup>1</sup> Road and Traffic Engineering Institute, College of Engineering, Zhejiang Normal University, Jinhua 321004, China

<sup>2</sup> Key Laboratory of Road and Traffic Engineering of the Ministry of Education, Tongji University, Shanghai 201804, China

\* Correspondence: yangq@zjnu.cn

**Abstract:** The study aims at investigating diffusion behaviors between virgin asphalt and recycled asphalt mastic (RAM) at an atomistic scale. Firstly, a mutual diffusion model of virgin asphalt–RAM considering the actual mass ratio of filler to asphalt binder (F/A) condition was developed by molecular dynamic (MD) simulation. Secondly, the indexes of relative concentration (RC), radial distribution function (RDF) and mean square displacement (MSD) were used to analyze the molecular arrangement characteristics of polar components in the diffusion processes at different temperatures. Then, the blending efficiency of virgin asphalt–RAM was evaluated by Fick’s second law and the binding energy. The results indicate that the reliability of the RAM model was validated by thermodynamics properties. The results of RC and RDF show that the diffusion direction of virgin asphalt–RAM is not changed by the presence of mineral fillers. However, it will inhibit the occurrence of diffusion behaviors, and the aggregation of molecules in the blending zone increases due to the adsorption of mineral fillers, which would become a barrier to molecular diffusion. The development of MSD indicates that the diffusion coefficients of molecules in both virgin–aged asphalt and virgin asphalt–RAM are on the rise with the increase in temperature. Compared with the virgin–aged asphalt, the molecular migration speed in virgin asphalt–RAM is relatively slow. According to Fick’s second law and the binding energy, diffusion behaviors are dominated by the nonpolar components. The existence of mineral fillers has the greatest effect on the nonpolar components in diffusion. It is suggested that rejuvenator containing more aromatic components should be added or the temperature controlled within 433.15–443.15 K to promote blending efficiency. The research results contribute to a deeper understanding about diffusion behaviors of virgin asphalt–RAM, serving as a benchmark for further study of rejuvenation using computational experiments.

**Keywords:** virgin asphalt–RAM; molecular dynamic; diffusion behaviors; blend efficiency; molecular arrangement; nanostructure



**Citation:** Chen, S.; Yang, Q.; Qiu, X.; Liu, K.; Xiao, S.; Xu, W. Use of MD Simulation for Investigating Diffusion Behaviors between Virgin Asphalt and Recycled Asphalt Mastic. *Buildings* **2023**, *13*, 862. <https://doi.org/10.3390/buildings13040862>

Academic Editor: Hang Lu

Received: 20 February 2023

Revised: 9 March 2023

Accepted: 22 March 2023

Published: 25 March 2023



**Copyright:** © 2023 by the authors. Licensee MDPI, Basel, Switzerland. This article is an open access article distributed under the terms and conditions of the Creative Commons Attribution (CC BY) license (<https://creativecommons.org/licenses/by/4.0/>).

## 1. Introduction

The asphalt pavement during long service inevitably enters a stage of both construction and maintenance resulting from the ever-increasing traffic loading and environmental corrosion, producing a considerable amount of reclaimed asphalt pavement (RAP). RAP can be recycled in pavement construction after mixing with virgin asphalt after a certain process of crushing and screening. Recently, many studies have supported the assumption that partial blending occurs between the virgin asphalt and aged asphalt (virgin–aged asphalt) around the surface of the reclaimed aggregate [1–3]. Through analyzing blending behaviors of virgin–aged asphalt deeply, the blending mechanism by which the asphalt binders would still maintain their original microstructures and keep the state of heterogeneous composite is interpreted. Nahar et al. [4] and Zhao et al. [5] explored a blending zone and discovered that virgin–aged asphalt began to co-mingle in the zone and became

homogeneous. Consequently, it is essential to investigate diffusion behaviors of virgin-aged asphalt for promoting the blending degree and homogeneous distribution in reclaimed asphalt mixtures.

Blending behavior can be defined as an interdiffusion process, which refers to the asphalt binder homogenization process after virgin asphalt and aged asphalt contact each other. Diffusion behaviors of virgin asphalt and regenerating agent in aged asphalt are the fundamental reason for promoting the regeneration of RAP. Several basic theories have been developed to explain diffusion behaviors of virgin-aged asphalt, including Fick's law [6], mass transfer and molecular dynamic (MD) theory [7]. Fick's law is beneficial to explain the changes in concentration over time and by location. Ding et al. [8] designed the diffusion simulation test of aged asphalt to virgin aggregate based on Fick's law and the Einstein–Stokes equation to evaluate the influence of mixing time, construction temperature, regeneration dose and amount of aged asphalt on the transfer efficiency of aged asphalt layers from RAP. Mass transfer theory describes mass transfer processes between liquid and solid or for two fluid phases. With the help of the mass transfer theory, Ma et al. [9] discussed the influencing factors of the effective regeneration rate of aged asphalt. Tao et al. [10] investigated the transfer mechanism between virgin asphalt and reclaimed aggregates in the mixing process. MD theory is considered to be the simulation of molecular microcosmic behavior during the blending process. The aging process is usually characterized by the increase in and accumulation of asphaltenes while the regeneration process mainly involves the molecular interaction occurring in the virgin-aged asphalt. Tang et al. [11] used MD technology to analyze the aggregation characteristics of asphalt molecules, which showed that the resin and oil molecules would promote the stability of the aggregation structure of asphaltene molecules. There exists difficulty in revealing the diffusion mechanism on account of the complex chemical structures and influencing factors of the asphalt, while the MD simulation is employed as an effective method to analyze diffusion behavior of virgin-aged asphalt and the regeneration efficiency of RAP.

With the wide application of RAP, many studies about the diffusion effect of virgin-aged asphalt have been carried out. Scholars proposed to adopt dynamic shear rheology (DSR) or a bending beam rheometer (BBR) to detect the rheological properties of asphalt binders [12,13]. In addition, gel permeation chromatography (GPC) or Fourier transform infrared spectroscopy (FTIR) has been used to study the chemical properties of asphalt binders. Ding et al. [14] explored the mixing effect and molecular aggregation between virgin and aged asphalt, and found that the interaction affected the performance of blended asphalt. To further understand remobilization phenomena which occur during the manufacture of reclaimed asphalt mixtures, the carbonyl distribution profile was used to monitor the aged asphalt migration [15]. Furthermore, through analyzing the extracted asphalt from mixtures, it was revealed that diffusion behaviors and blending efficiencies are significantly affected by the methods, temperatures and duration of the processes [16–18]. Optical methods were used to measure the distribution of elements and make images of the blending zone, such as a fluorescence microscope (FM), scanning electron microscope (SEM), computer tomography (CT scan) and X-ray scanning [19–21]. Some scholars combined micro and macro perspectives to analyze the morphology and properties changes in virgin-aged asphalt fusion and quantified the microstructure by indexes of roughness, carbonyl and sulfoxide [22,23]. As mentioned above, these studies confirmed that it has become a research trend to characterize diffusion behaviors at a microscopic scale. It is worth noting that since the diffusion processes between virgin and aged asphalt are particularly sophisticated, further monitoring of the diffusion processes and explaining the diffusion mechanism with more advanced testing approaches are vital to improve the performance of reclaimed asphalt mixtures.

MD simulation refers to the use of statistical mechanics-based theoretical methods and computational techniques to model the behaviors of molecules under different conditions, which is used to record time trajectories of atoms. MD simulation has been widely employed to model the diffusion motion in the field of asphalt materials, thereby creating a chance to

reveal the diffusion mechanism of virgin–aged asphalt from nanostructure characteristics and molecular arrangements, which is difficult to study experimentally. Mean square displacement (MSD), cohesive energy density (CED) and relative concentration (RC) were used to characterize the diffusion behavior of virgin–aged asphalt. Studies have shown that the diffusion direction of the virgin–aged asphalt was mainly confirmed from the virgin asphalt to the aged asphalt [24]. For instance, Huang et al. [25] demonstrated that the increase in temperature is beneficial to the diffusion of asphalt on the aggregate surface. In the diffusion process, van der Waals force was the main factor to drive the movement of asphalt molecules on the aggregate surface. Xu et al. [26] proved that small or catenarian molecules diffuse faster than the network structures. Additionally, Ding et al. [14] investigated mixing effect and molecular aggregation between virgin and aged asphalt, indicating that the molecular aggregation was more significant for fractions with different chemical structures. In addition, to further describe the interdiffusion process, the Fickian diffusion equation has been employed in the quantitative evaluation of diffusion efficiency [27,28]. As mentioned above, these achievements enormously enriched the MD simulation to be applied in the field of asphalt regeneration and made great contributions for understanding diffusion behaviors and interaction mechanism of virgin–aged asphalt. However, the MD method still has limitations on establishing the molecular model that approaches the actual situation to deeply understand the diffusion mechanism. Actually, the aged asphalt does not exist alone in the dispersed system of reclaimed asphalt mixtures, but is coated on the surface of the reclaimed aggregate in the form of recycled asphalt mastic (RAM), which makes the diffusion processes more complicated. However, the performance of recycled materials measured in laboratory tests may deviate from the actual performance if the actual diffusion situation is not taken into account. Therefore, it is urgent to establish a realistic molecular model and deeply study diffusion behaviors between virgin asphalt and RAM (virgin asphalt–RAM) to effectively evaluate the regeneration effect of RAP.

Consequently, the objective of this research is to investigate the nanostructure characteristics and molecular arrangements of polar components between virgin asphalt and RAM during the diffusion process through MD simulation and quantitatively evaluate their blending efficiencies. Specifically, this study aims to:

- (1) Establish molecular models for the characterization of RAM under actual F/A conditions and verify them by evaluating thermodynamic parameters of virgin asphalt, aged asphalt and RAM.
- (2) Construct a mutual diffusion model of virgin asphalt–RAM to clarify the diffusion mechanism from the perspectives of nanostructure characteristics and molecular arrangements based on relative concentration, radial distribution function and mean square displacement.
- (3) Use Fick's second law and binding energy to quantitatively evaluate blending efficiencies of virgin asphalt–RAM.

Accordingly, the study gives a comprehensive perspective of the diffusion behaviors and mechanism of virgin asphalt–RAM, and provides support to effectively evaluate the regeneration effect of RAP and improve the performance of reclaimed asphalt mixtures.

## 2. Methods and Model Development

### 2.1. Molecular Structures

Asphalt derived from crude oil is a mixture of hydrocarbons that contains millions of molecules, and it would be impractical to model all of them. Therefore, scholars have sought to find typical structures which could represent the various molecules in bitumen. Li and Greenfield [29] established a 12-component asphalt model about virgin asphalt, which is close to asphalt in reality. Qu et al. [30] added various numbers of carbonyl (C = O) and sulfoxide (S = O) to the asphalt to characterize asphalt with different aging degrees. Cui et al. [31] carried out an aging experiment using 70# asphalt which was provided by the company SK, and calculated the quantity of each molecule by means of SARA and FTIR experiments, then constructed the model as close as possible to real asphalt. All models

used in this study were derived from Cui's research results [32]. The molecular structures are illustrated in Figure 1. The main changes in chemical structures in the aging process of asphalt are shown in Figure 2.

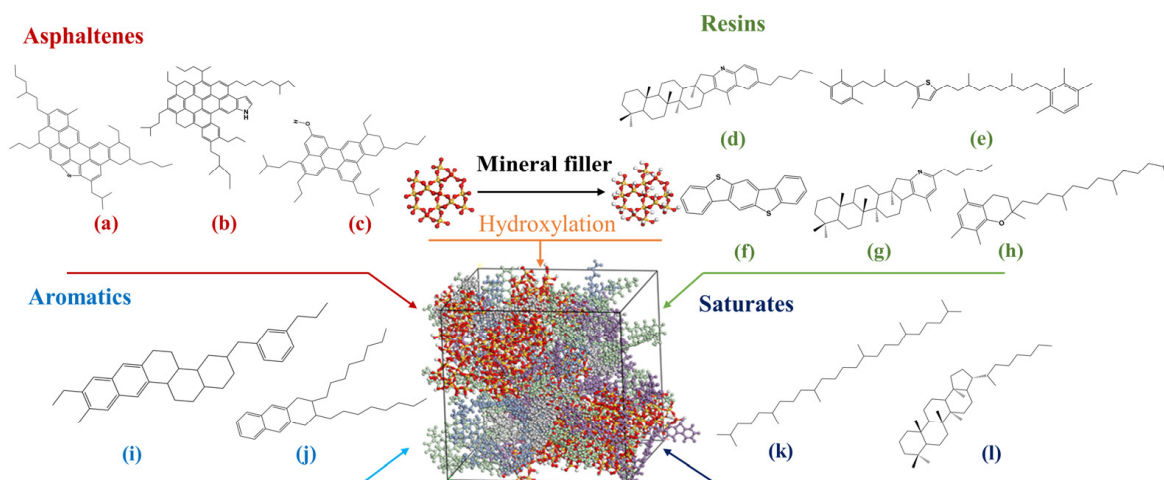


**Figure 1.** Molecular structures used in the 4-component model of asphalt. Asphaltenes: (a) Thiophene, (b) Pyrrole, (c) Phenol; Resins: (d) Quinolinhopane, (e) Thio-isorenieratane, (f) Benzobisbenzothio-*phene*, (g) Pyridinohopane, (h) Trimethylbenzene-oxane; Aromatics: (i) PHPN, (j) DOCHN; Saturates: (k) Squalane, (l) Hopane.

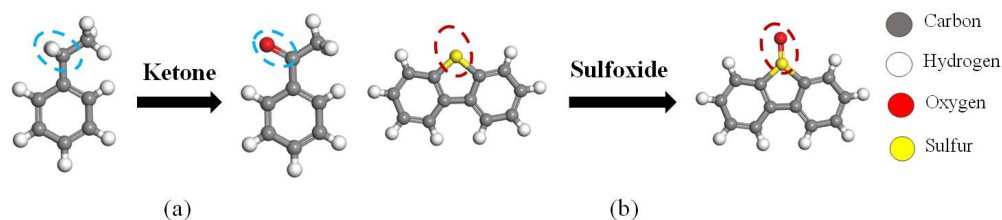


**Figure 2.** Illustration of major oxidative products in asphalt: (a) Ketone group; (b) Sulfoxide group.

Silica is a major component of most mineral fillers, therefore, silica was selected as a simplified mineral filler to be added to the asphalt model [33]. Firstly, an alpha-quartz supercell crystal structure was created based on the structure database of Materials Studio software. Secondly, after the atoms beyond the radius of 5 Å were discarded, spherical nanoclusters with oxygen atoms as cut-off atoms were formed. Finally, in order to balance the charge of the sphere nanocluster, H atoms were added to the surface of oxygen atoms. As shown in Figure 1, 16 Si atoms, 50 O atoms and 24 H atoms form the sphere nanocluster.

The RAM model was constructed by packing mineral fillers and asphalt molecules, as shown in Figure 1. Based on the Superpave volume mixture design method, the filler-to-asphalt mass ratio of 0.6–1.2 was recommended. The reasons for adopting the F/A of 1.2 are presented as follows: (1) previous tests proved that the asphalt mastic with 1.2 F/A displayed better interaction behaviors with aggregates, which meant superior road performance [34]. (2) An F/A no more than the critical volume fraction of 40% can avoid particle structuring. The purpose of this study is to investigate the diffusion behavior of virgin asphalt and RAM, and the F/A of 1.2 was chosen.

## 2.2. Bulk Asphalt Models

The models of virgin asphalt, aged asphalt and RAM with 1.2 F/A were established. The saturate, aromatic, resin and asphaltene (SARA) components consist of molecules with disparate chemical compositions, as illustrated in Table 1. All models were constructed at a temperature of 298.15 K, and the initial density was 0.6 g/cm<sup>3</sup>. After establishing the virgin asphalt model, an equilibrated molecular configuration was obtained by using a

smart algorithm that performed 5000 geometric calculations on the system. Then, in order to eliminate unreasonable structures in the model, an annealing procedure was carried out for eight cycles wherein the temperature was ramped from 400 K to 800 K under the N: constant particle number, V: constant volume, T: constant temperature (NVT) ensemble. After that, the model was subjected to dynamic equilibration through the N: constant particle number, P: constant pressure, T: constant temperature (NPT) ensemble at 298.15 K for 500 ps to obtain a structure that was similar to the actual state. Finally, an optimization step was performed for 500 ps at 298.15 K under the NVT ensemble and, after this stage, the final structure with volume and energy stability was obtained. In all the above operations, the last structure was selected as the next initial state. The operation procedure of MD simulation in this study is shown in Figure 3.

**Table 1.** Molecular structure characteristics of asphalt components.

SARA Components	Molecular Name	Virgin Asphalt		Aged Asphalt			
		Molecular Number	Molecular Formula	Molecular Number	Molecular Formula	C = O	S = O
Saturates	Squalane	8	C <sub>30</sub> H <sub>62</sub>	6	C <sub>30</sub> H <sub>62</sub>	0	0
	Hopane	7	C <sub>35</sub> H <sub>62</sub>	8	C <sub>35</sub> H <sub>62</sub>	0	0
Aromatics	PHPN	14	C <sub>35</sub> H <sub>44</sub>	12	C <sub>35</sub> H <sub>40</sub> O <sub>2</sub>	2	0
	DOCHN	15	C <sub>30</sub> H <sub>46</sub>	12	C <sub>30</sub> H <sub>44</sub> O	1	0
Resins	Pyridinohopane	2	C <sub>36</sub> H <sub>57</sub> N	4	C <sub>36</sub> H <sub>55</sub> NO	1	0
	Thio-isorenieratane	2	C <sub>40</sub> H <sub>60</sub> S	3	C <sub>40</sub> H <sub>58</sub> O <sub>2</sub> S	1	1
	Trimethylbenzene-oxane	2	C <sub>29</sub> H <sub>50</sub> O	2	C <sub>29</sub> H <sub>48</sub> O <sub>2</sub>	1	0
	Quinolinohopane	1	C <sub>40</sub> H <sub>59</sub> N	3	C <sub>40</sub> H <sub>57</sub> NO	1	0
	Benzobisbenzothiophene	13	C <sub>18</sub> H <sub>10</sub> S <sub>2</sub>	16	C <sub>18</sub> H <sub>10</sub> OS <sub>2</sub>	0	1
Asphaltenes	Phenol	2	C <sub>42</sub> H <sub>54</sub> O	3	C <sub>42</sub> H <sub>50</sub> O <sub>3</sub>	2	0
	Pyrrrole	1	C <sub>66</sub> H <sub>81</sub> N	1	C <sub>66</sub> H <sub>73</sub> NO <sub>4</sub>	4	0
	Thiophene	2	C <sub>51</sub> H <sub>62</sub> S	3	C <sub>51</sub> H <sub>58</sub> O <sub>3</sub> S	2	1

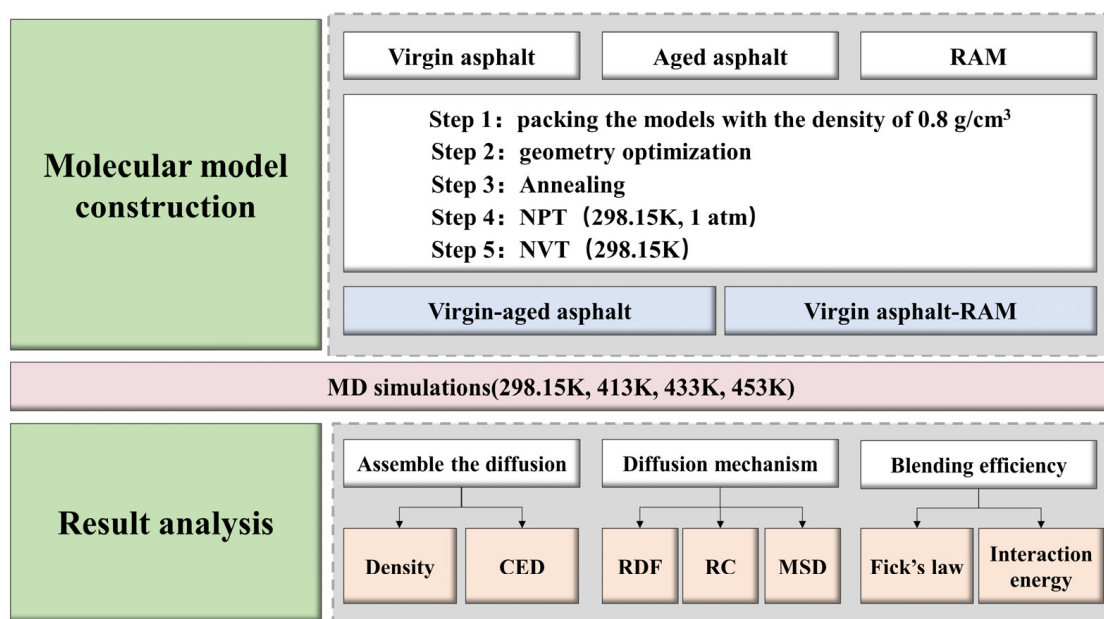


**Figure 3.** Flowchart of MD simulation conducted in this study.

### 2.3. Mutual Diffusion Model

The diffusion efficiency of virgin–aged asphalt determines whether uniform recycled asphalt can be formed, which affects the performance of recycled asphalt. In order to

investigate the influence of temperature and mineral filler on the diffusion efficiency, a double-layer model was established.

The two kinds of mutual diffusion models with double layers are shown in Figure 4. The optimization process of the two models is consistent. Using the Build Layer command, we set Layer1 to virgin asphalt and Layer2 to aged asphalt/RAM, without adding a vacuum layer between the two layers. After establishing the double-layer model, a geometric calculation with 5000 cycles was conducted on the system, then an annealing simulation was carried out under the NVT ensemble with eight cycles of temperature from 400 K to 800 K. Finally, simulation was implemented under the NPT and NVT ensembles successively for 500 ps at the temperatures of 298.15 K, 415.15 K, 433.15 K, 453.15 K, to observe the interdiffusion process of virgin and aged asphalt at the same time.

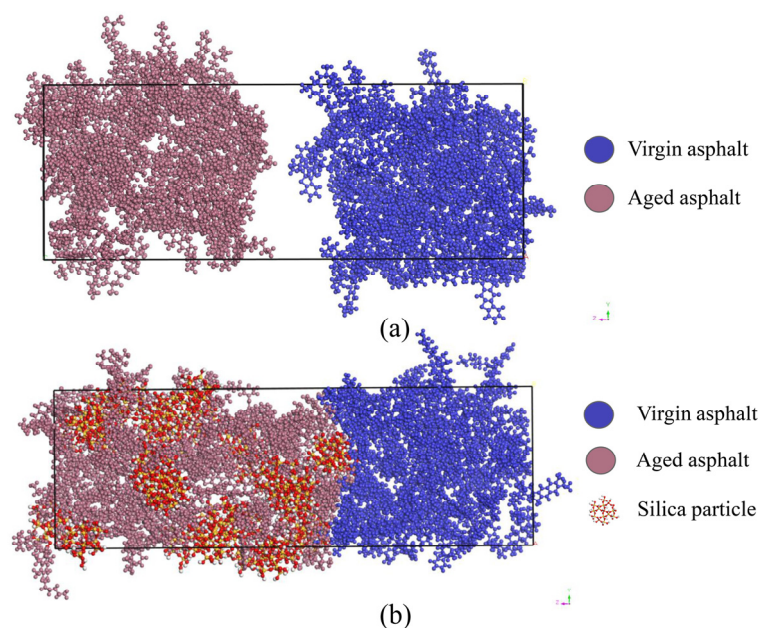


**Figure 4.** Mutual diffusion model: (a) virgin–aged asphalt; (b) virgin asphalt–RAM.

#### 2.4. Force Field and Simulation Details

In this study, all the stages of molecular modeling and dynamic simulation were implemented by commercial software, Materials Studio 8.0. During the simulation, a condensed-phase optimized molecular potentials for atomistic simulation studies (COMPASS II) force field was adopted to calculate the bond and nonbond interactions of all atoms in the system, which was widely applied to organic and inorganic small molecules and polymers. It also has been proved that it could predict molecular, molecular liquid and crystal properties accurately. With the method of an atom-based summation, a cut-off distance was selected as 15.5 Å for the van der Waals interaction. As for the electrostatic interaction, a 6 Å cutoff distance was selected with the help of the Ewald summation method. In all simulation processes, a time step of 1 fs was set, and dynamic trajectory and other statistical data were output every 1000 steps. The Nosé–Hoover thermostat was employed to control the temperature and the Berendsen barostat was adopted to balance the pressure.

### 3. Results and Discussion

#### 3.1. Model Validation

##### 3.1.1. Density

Density is a fundamental thermodynamic characteristic of asphalt binder, which can be employed to identify reasonability of the molecular models and force field set in a simulation. The densities of virgin asphalt, aged asphalt and RAM models are shown in Figure 5. The densities of virgin asphalt, aged asphalt and RAM models gradually

become stable after 50 ps, around  $0.98 \text{ g/cm}^3$ ,  $1.02 \text{ g/cm}^3$  and  $1.40 \text{ g/cm}^3$ , respectively. Obviously, the density of aged asphalt is higher than that of virgin asphalt. By analysis, the density of virgin asphalt increases due to the introduction of oxygen atoms during the oxidative aging process. In particular, the density of RAM increases by 37.25% after adding the filler particles. According to Table 2, the results of densities have a great agreement with the previous experimental and simulation results, which proves the rationality of the simulation.

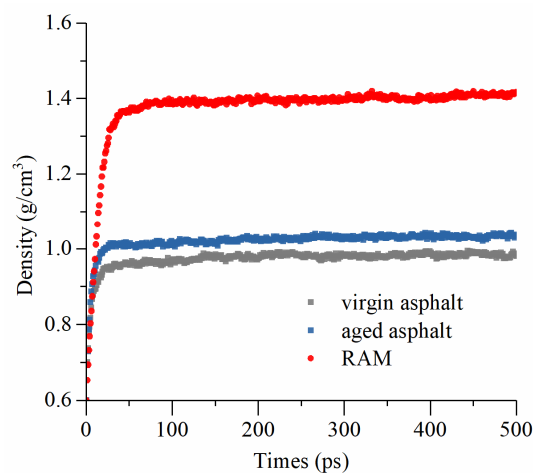


**Figure 5.** Densities of three types of asphalt models.

**Table 2.** Calculated results of virgin asphalt in MD simulations.

Properties	Calculated Results	Results in the Literature
Density (298.15 K)	0.98	0.92 (Long et al. [35]); 0.997 (Khabaz and Khare [36]); 0.981 (Gao et al. [37])
Cohesive energy density ( $10^8 \text{ J/m}^3$ )	3.20	3.32 (Xu and Wang [38]); 3.21 (Wang et al. [39])

### 3.1.2. Cohesive Energy Density

Cohesive energy density (CED) can assess the intermolecular bonding strength, which refers to the energy required to remove a given molecule from its nearest neighbor. The CED results calculated from virgin asphalt, aged asphalt and RAM models are illustrated in Figure 6. Total CED consists of van der Waals energy and electrostatic energy, in which van der Waals energy accounts for much more than electrostatic energy, indicating that van der Waals energy plays a major role. CED of aged asphalt is higher than that of virgin asphalt. The reason is that the polarity of asphaltene is higher than that of other components, while there are more asphaltenes in aged asphalt. Moreover, the CED of RAM is also higher than that of aged asphalt. By analysis, the silica particles strengthen the intermolecular interaction of the asphalt. A high CED value indicates that the diffusion ability of molecules in this model is weak, and suggests that external molecules struggle to diffuse into the model. In addition, adding silica particles increases the percent of electrostatic energy and decreases van der Waals energy. The reason is that there is a residual charge on the silicon dioxide atom, and the electrically neutral silicon dioxide molecule will interact due to Coulomb electrostatic interaction. The molecular configuration of the components in the virgin asphalt changes due to the presence of silica molecules, resulting in a decrease in van der Waals energy. The density and CED results of all models are in great agreement with previous studies, as shown in Table 2 [32], that is, to a certain extent, the molecular model and force field selected are proper and reliable. Therefore, the RAM model constructed by this method and described in this paper is also reliable for subsequent analysis.

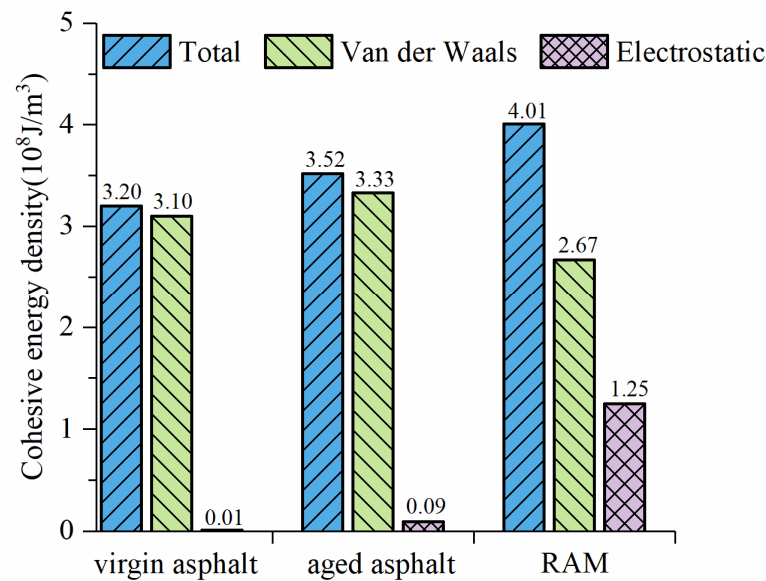


**Figure 6.** CED values for three types of asphalt models.

### 3.2. Nanostructure Characteristics of Diffusion Behavior

#### 3.2.1. Relative Concentration

The relative concentration distribution of asphalt components in the virgin asphalt–RAM can accurately describe the distribution characteristics of polar components under the adsorption of silica particles in the diffusion process, and further reveal the diffusion direction and migration depth. According to Equations (1) and (2), the relative concentration and plate concentration of particles can be obtained, respectively.

$$RC_i = \frac{C_i}{C_{bulk}} \quad (1)$$

$$C_i = \frac{N_i}{V_i} \quad (2)$$

where  $RC_i$ ,  $C_i$  and  $V_i$  represent the relative concentration, the concentration and the volume of the slab  $i$ , respectively;  $N_i$  and  $C_{bulk}$  represent the quantity of particles in the slab  $i$  and the bulk concentration, respectively.

In order to analyze relative concentration, the range from 0 ps to 500 ps of the diffusion process in the OZ direction is selected as the object. Figure 7 shows the relative concentration distribution of virgin–aged asphalt and virgin asphalt–RAM at 433.15 K. As can be seen from Figure 7, virgin asphalt–RAM is distributed on both sides of the model when the relative concentration curve is at 0 ps, and no diffusion occurs. At 500 ps, the covering length of virgin asphalt changes from 0–45 Å to 0–58 Å, and the covering length of RAM changes from 45–120 Å to 42–100 Å, manifesting that substances on both sides of the model diffuse into to each other over time, and the main diffusion is from virgin asphalt to RAM. In the middle region, the relative concentration increases from the initial 0 to about 1, indicating that virgin asphalt is fused with RAM. The virgin–aged asphalt and virgin asphalt–RAM models show the same diffusion trend, which means the presence of silica particles does not change the diffusion direction. Compared with Figure 7a,b, after 500 ps simulation, the molecular overlap on both sides in (a) is larger than that in (b), demonstrating that the presence of silica particles causes a decrease in the diffusion depth of virgin asphalt–RAM. Additionally, the covering length of virgin asphalt decreased by 16%, while that of aged asphalt decreased by 21%, revealing that the inhibition effect of silica particles on the diffusion of aged asphalt is more obvious than that of virgin asphalt.

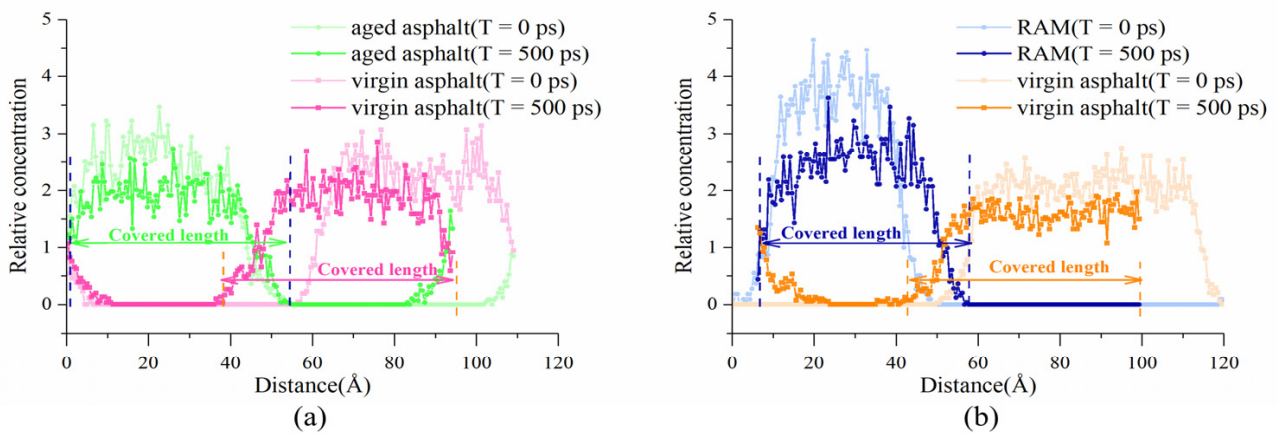


**Figure 7.** Relative concentration distribution at 433.15 K: (a) virgin-aged asphalt; (b) virgin asphalt–RAM.

The relative concentration distribution of SARA components in the z direction is illustrated in Figure 8. As far as virgin–aged asphalt is concerned, the relative concentrations of SARA components are mainly distributed around 1.0%. The asphaltene shows the most “narrow and high” peak with RC of 2.0%. For the curve of resin, the highest peak value is 1.5%, and the overall distribution is wide. This phenomenon indicates that the asphaltenes of virgin–aged asphalt are aggregated during the diffusion process. Compared with asphaltene, the RC curve of resin covers the distribution range of asphaltene, and displays a more uniform distribution.

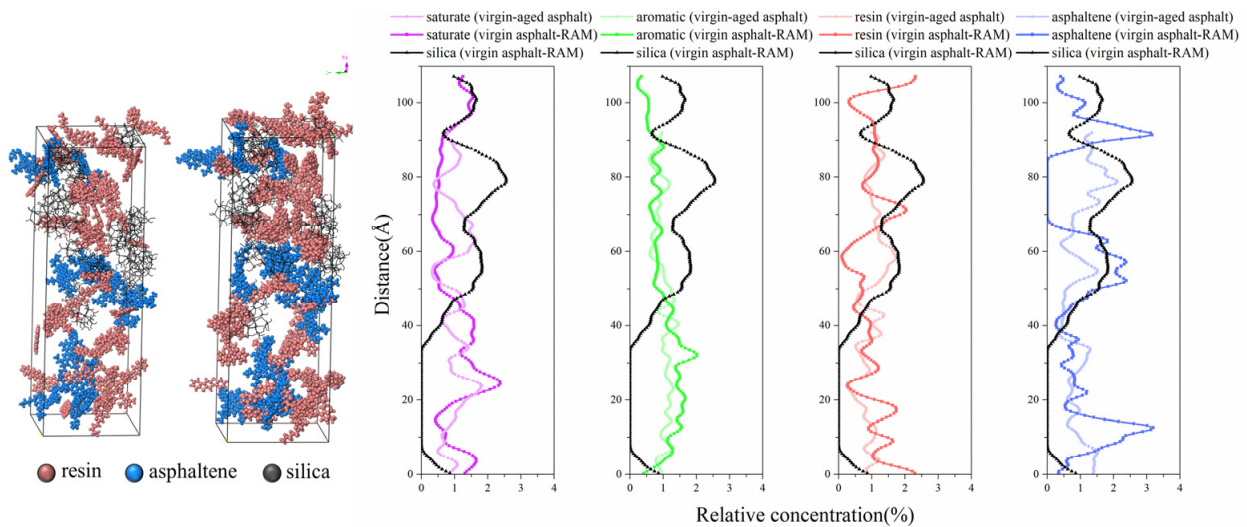


**Figure 8.** Relative concentration distribution of SARA components of asphalt.

As for virgin asphalt–RAM, the peak value of RC of asphaltene is increased by the silica particles from 2.0% to 3.3%. The peak value of resin increases from 1.5% to 2.4%, presenting the same change pattern as other components. Affected by the silica particles, the curve of polar components fluctuates greatly with the concentration range, expanding from 0.5–1.5% to 0–3%, while the aromatic fraction is almost unchanged, which reflects that the polar components are greatly affected by silica particles.

Additionally, in the blending zone around 50–60 Å, the distribution curves of polar components show a similar pattern to that of silica particles, confirming that polar components form a large number of aggregates in the blending zone and gather around the silica particles.

By comparing Figure 9a,b, due to the presence of silica particles, the asphaltene in virgin asphalt is adsorbed onto the silica particles in RAM. The asphaltene in RAM is

adsorbed onto silica particles and moves in the direction of virgin asphalt along with silica particles. In addition, the agglomeration of asphaltene is more obvious, and the resin surrounds the aggregates, which leads to the increase in relative concentration in the blending zone. Most aggregates accumulate in the blending zone, forming a compact structure, which prevents molecules on both sides from moving toward each other to a certain extent, and only small molecules can diffuse by crossing the void.

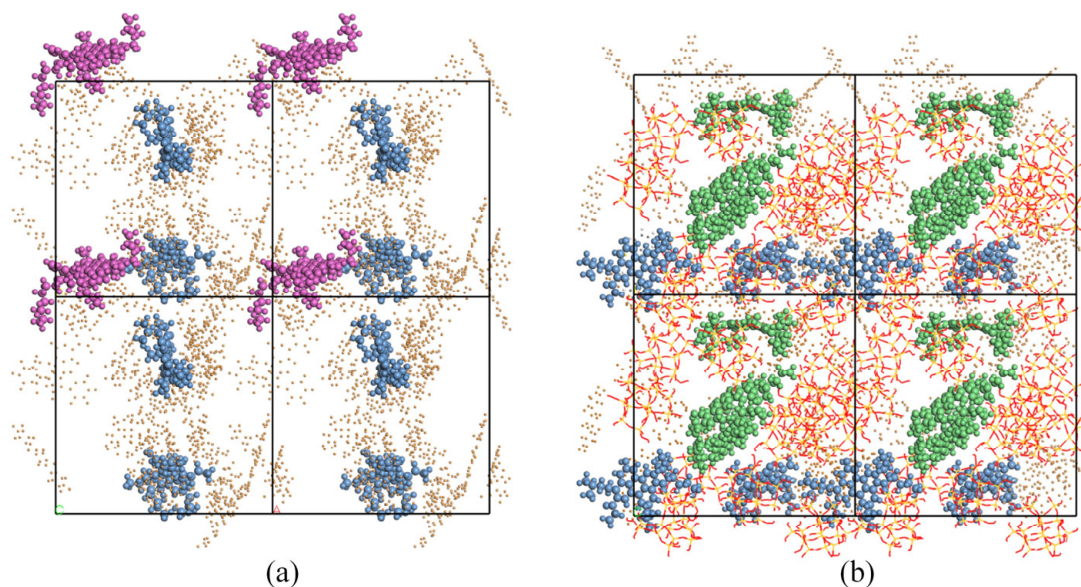


**Figure 9.** Nanostructure of asphaltene aggregation in blending zone: (a) virgin-aged asphalt; (b) virgin asphalt–RAM ( $2 \times 2$  repetitive units, blue refers to phenol molecules; green refers to thiophene molecules; purple refers to pyrrole molecules; yellow refers to resin molecules).

### 3.2.2. Radial Distribution Function

Previous research shows that diffusion behaviors of asphalt are determined by the diffusion ability as well as influenced by the properties of the diffusion receptor [40]. The effect of diffusion behavior and blend efficiency can be effectively illustrated by characterizing the nanostructure and molecular arrangements of polar components. RDF is an important index to characterize the molecular aggregation and nanostructure arrangement. In mathematics, RDF represents the ratio of the local density of the reference molecule to the bulk density of the models, which can reflect the ordering and stacked state of the molecule distribution. At a certain distance, molecular aggregation can be represented by the characteristic peaks of the RDF curve. Equation (3) is the calculation formula of RDF function.

$$g(r) = \frac{1}{\rho 4\pi r^2 \delta r} \times \frac{\sum_{t=1}^T \sum_{j=1}^N \Delta N(r \rightarrow r + \delta r)}{N \times T} \quad (3)$$

where  $n$ ,  $r$ ,  $T$ ,  $\delta r$ ,  $\rho$  and  $\Delta N$  represent the total number of molecules, the radius from the target particle, the total calculation time (ps), the designed difference in the distance, the density of the models and the number of the molecules within the interval of  $r \rightarrow r + \delta r$ , respectively.

RDF can characterize and explain the colloidal structure and asphaltene aggregation. Figure 10 shows the molecular arrangements of different models for asphaltene–asphaltene and asphaltene–resin pairs at 298 K, respectively. It can be seen that the RDF curves present the characteristic of sharp oscillation peaks in the range of 0–3 Å. When  $r$  is in the range of 3–5 Å, the change in the amplitude is unobvious. As  $r$  exceeds 5 Å, the curve of RDF is stabilized and the value of RDF tends to 1. These results reveal that the particles are distributed irregularly.

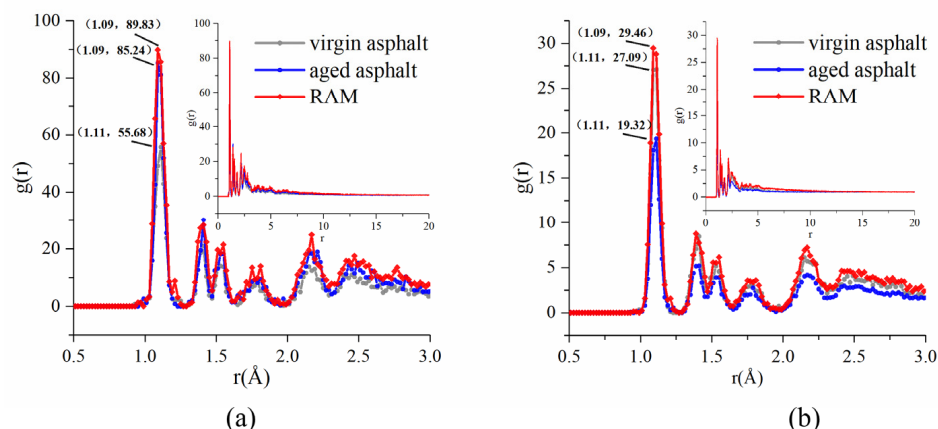


**Figure 10.** RDFs of SARA components: (a) asphaltene–asphaltene; (b) asphaltene–resin.

It can be seen from Figure 10a that the RDF peak of the asphaltene pair after experiencing oxidative aging rises sharply from the initial state (1.11, 55.68) to a point (1.09, 85.24). The results show that oxidative aging seriously increases the self-aggregation of asphaltenes, resulting in the change in internal structure of the asphaltene pair. By analysis, it is seen that the oxidative aging strengthens the polarity and aromaticity of asphalt molecules, thus leading to the enhancement of the intermolecular association and interaction force [41]. However, the peak value of the asphaltene–resin pair in aged asphalt is lower compared with that in virgin asphalt, as illustrated in Figure 10b. The results represent that oxidative aging attenuates the aggregation of asphaltene and resin, and decreases the compatibility of asphaltene in resin.

As shown in Figure 11, to clearly demonstrate the effect of silica particles on the polar components during the diffusion process of virgin asphalt–RAM, the molecular structure of the polar components of virgin asphalt, aged asphalt and RAM is extracted. Apparently, as shown in Figure 11b, the oxidized asphaltene molecules interact with each other to form a dense parallel stacked structure, which comes down to the  $\pi$ – $\pi$  interaction between benzene rings. As shown in Figure 11c, the incorporation of silica particles results in a relatively large number of stacked structures. The asphaltene molecules are stacked around the silica particles and evenly dispersed among the resin molecules. Moreover, compared to the aged asphalt, the stacking distance between each layer of molecules is narrowed and the agglomeration trend of polar asphaltenes is accelerated, which may be caused by the adsorption of silica particles on asphaltene and the promotion of combination between asphaltene and resin to form a compact structure.

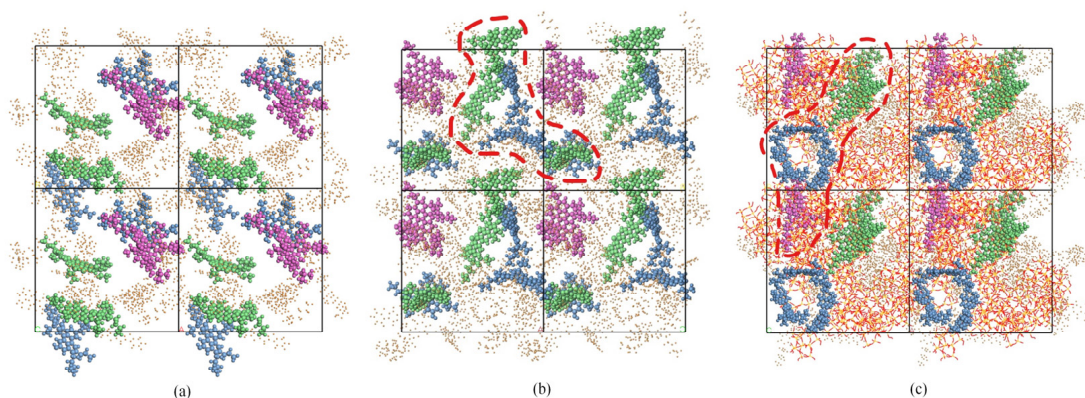


**Figure 11.** Illustration of the self-aggregation of asphaltenes in asphalt: (a) virgin asphalt; (b) aged asphalt; (c) RAM (2 × 2 repetitive units, blue refers to phenol molecules; green refers to thiophene molecules; purple refers to pyrrole molecules; yellow refers to resin molecules).

### 3.2.3. Mean Square Displacement

Mean square displacement (MSD) can be used to characterize the components' mobility in the diffusion process. As identified in Equation (4), MSD is a function about variability of the atomic positions over time. As shown in Equations (4) and (5), the diffusion coefficient ( $D$ ) of molecules is concretely calculated by the slope of the MSD curve based on the Einstein equation.

$$MSD = \langle (r_i(t) - r_i(0))^2 \rangle \quad (4)$$

$$D = \frac{1}{6N} \lim_{t \rightarrow \infty} \frac{d}{dt} \sum_{i=1}^N \langle |r_i(t) - r_i(0)|^2 \rangle \quad (5)$$

where  $r_i(0)$  represents the position vector of particle  $i$  at the initial time;  $r_i(t)$  represents the position vector of particle  $i$  at time  $t$ ; and  $\langle \rangle$  indicates that the squared magnitude of this vector is averaged over many such time intervals.

Figure 12 shows the MSD–time curves of SARA components at 298 K, respectively. It is also observed that the MSD curve of SARA components of the oxidation aged asphalt is below that of virgin asphalt in all the models. The reason is that the molecular polarity increases due to the high oxidation of aged asphalt during its service period, resulting in a decrease with the content of nonpolar components and an increase with the content of polar molecules in aged asphalt, and a prominent increase in the self-aggregation behavior observed in the RDF curve. Therefore, the fluidity of each component of aged asphalt is significantly reduced. After incorporating the silica particles, the MSD curve of RAM shifts downward, and the results reflect that the silica particles impede the diffusion extent of components.

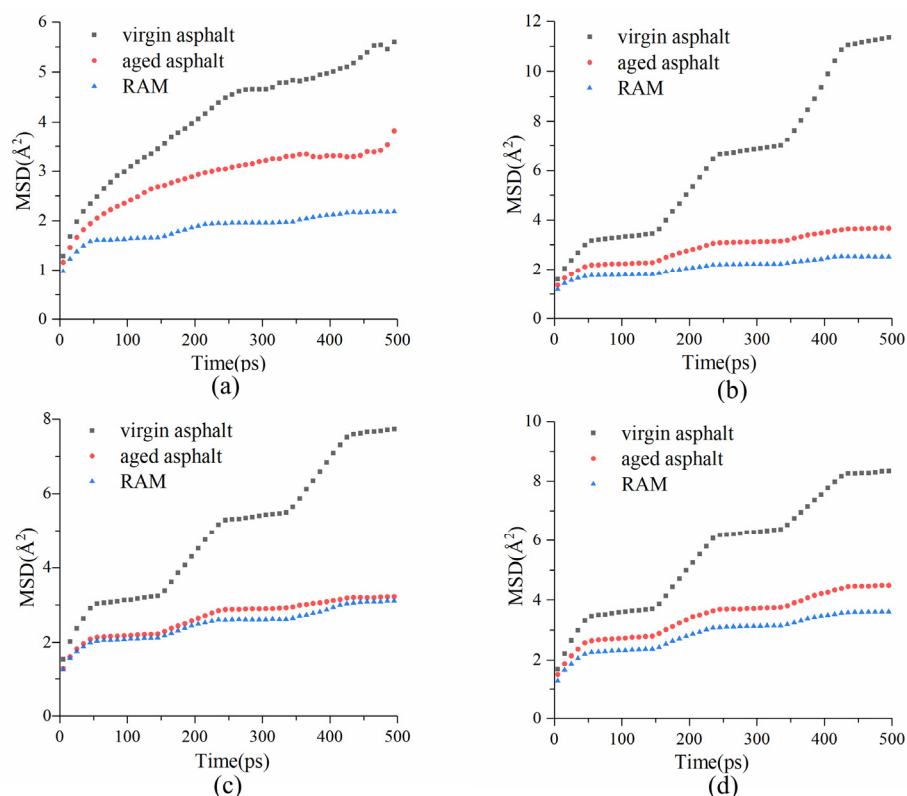


**Figure 12.** MSDs of SARA components: (a) asphaltene; (b) resin; (c) aromatic; (d) saturate.

The free volume can be used to describe the space within which molecules can move during the diffusion of molecules. The free volume is the part of the total volume that is not occupied by molecular chains and is scattered as tiny holes. As shown in Figure 13c, the FFV of RAM is relatively small at 32.1%, which means it cannot provide enough space

for molecule diffusion. The reason is that as molecules gather around the silica particles, internal voids and diffusion channels become crowded. This phenomenon would impede the flow of the nonpolar component, which is consistent with the above test results.

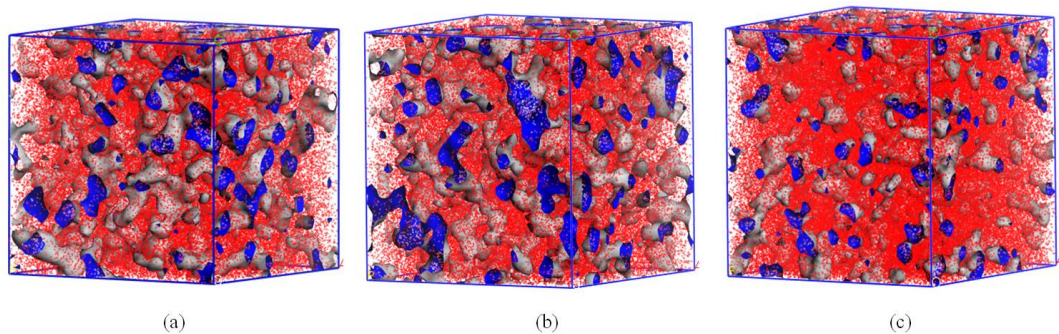


**Figure 13.** Free volume distributions among asphalts: (a) virgin asphalt (37.3%); (b) aged asphalt (36.4%); (c) RAM (32.1%) (occupied volume: red; free volume: blue; Connolly surface: gray).

According to Equation (5), diffusion coefficients of SARA components can be obtained and they are shown in Figure 14. Molecular weight determines the distinctive molecular mobility of different components. Molecular weight determines diffusion rates of SARA components of the two asphalts under the action of intermolecular forces and thermal movement. Saturate has the fastest diffusivity, followed by aromatic and resin, induced by the smallest molecular weight and simplest molecular structure. On the contrary, asphaltene with large molecular weight and complex configuration possesses the slowest migration velocity, and tends to self-association because of  $\pi$ - $\pi$  interaction between benzene rings. Contrasting Figure 14a,b, as the temperature increases, the mobility of the whole model also increases, and the change in the virgin asphalt–RAM is not obvious compared with the virgin–aged asphalt. It is observed that adding silica particles reduces the diffusivity of SARA fractions significantly. The decrease in the saturate fraction is 70%, and the decrease in asphaltene is only 17%. Especially at high temperature, silica particles have a great influence on the migration of nonpolar molecules. The presence of silica particles can reduce diffusion rates of SARA components, but the order of self-diffusion rates does not change.

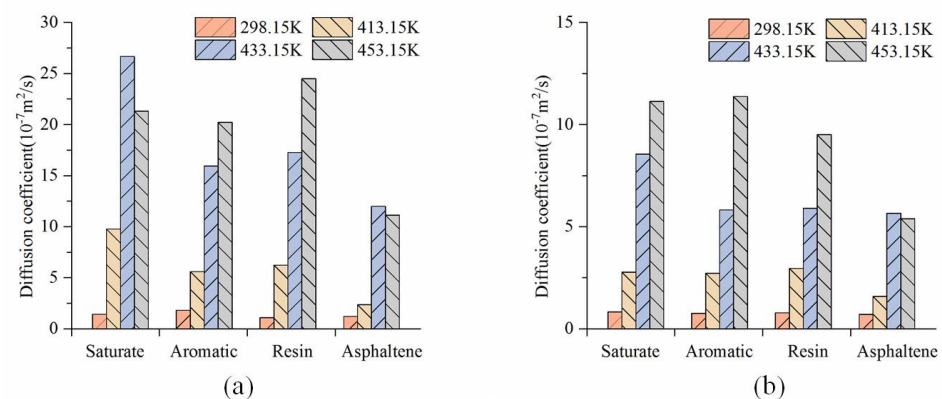


**Figure 14.** Self-diffusion coefficients of components at different temperatures: (a) virgin-aged asphalt; (b) virgin asphalt–RAM.

### 3.3. Quantitative Evaluation of Diffusion Efficiency

#### 3.3.1. Binding Energy

In virgin asphalt–RAM, the binding energy can reflect the strength of the interaction of asphalt components and the interaction between silica particles and asphalt components. At a certain temperature, diffusion behaviors of molecules are affected by attraction or

repulsion of components. The binding energy  $E_{\text{binding}}$  for each component of asphalt can be used to evaluate the promotion of the diffusion of macromolecules, which is defined as Equation (6) [41]. Positive values manifest attraction, while negative values indicate repulsion. The energies of SARA components of virgin asphalt with aged asphalt or RAM were extracted, and calculated according to the above results, respectively.

$$E_{\text{binding}} = E_{\text{component } a} + E_{\text{component } b} - E_{\text{composites } ab} \quad (6)$$

where  $E_{\text{component } a}$ ,  $E_{\text{component } b}$  and  $E_{\text{composites } ab}$  represent the energy of  $a$  component, kcal/mol, the energy of  $b$  component, kcal/mol, and the energy of a composite system containing both  $a$  and  $b$  components, kcal/mol, respectively.

Figure 15 exhibits the binding energies among SARA components of virgin asphalt with aged asphalt (without silica) or RAM (with silica). As shown in Figure 15, all of the calculated  $E_{\text{binding}}$  values are positive, indicating that the intermolecular attraction promotes the diffusion of components. For virgin–aged asphalt, the binding energy between aromatics and aged asphalt is the highest, followed by saturates, suggesting that the nonpolar components play a major role in the diffusion process by having a great attraction. However, the asphaltene and the resin have inferior binding energy with aged asphalt, which means that the diffusion ability is relatively poor.

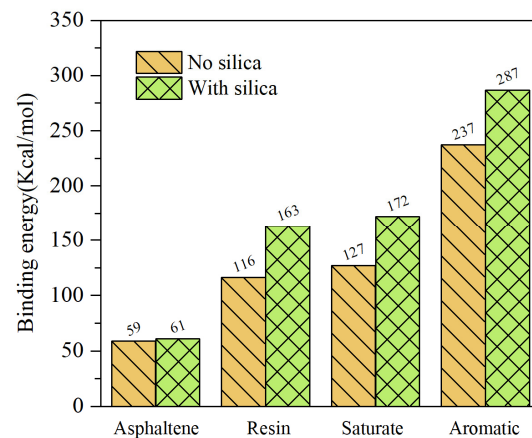


**Figure 15.** Binding energies among SARA components of virgin asphalt with aged asphalt (without silica) and RAM (with silica).

Additionally, it is also found that the existence of silica particles has a similar adjustment effect on the binding energy, which means that the binding energies between SARA components of virgin–aged asphalt have different degrees of promotion. The results show that the presence of silica particles obviously promotes the  $E_{\text{binding}}$  of aromatics and aged asphalt by 21.10%, which was the most significant improvement. Meanwhile, the  $E_{\text{binding}}$  between asphaltene and aged asphalt increases by 3.39%. It is probably due to the voids inside aged asphalt being penetrated by the silica particles, which partially plays the role of building a strong interaction of oxidized asphalt. Nevertheless, the gravitational force between the macromolecules of virgin–aged asphalt does not increase obviously, which has almost no effect on the movement of macromolecules in virgin asphalt to the aged asphalt. Consequently, it is found that the silica particles inhibit the diffusion behavior of virgin–aged asphalt by enhancing the interaction among the components in the aged asphalt and weakening the attraction between the aged asphalt and macromolecules in virgin asphalt.

Figure 16 shows binding energies of the virgin–aged asphalt and virgin asphalt–RAM at different temperatures. It is observed that when the temperature increases, the binding energy of virgin–aged asphalt shows a linear pattern of first increasing and then decreasing. The maximum value appears at 433.15 K, indicating that the interaction between components is the strongest at this temperature, and the same trend is observed

in virgin asphalt–RAM. Compared with virgin–aged asphalt, the binding energy of virgin asphalt–RAM at each temperature is higher than that of virgin–aged asphalt, which may be due to the presence of silica particles that enhances intermolecular interaction in aged asphalt. The binding energies of both models present the maximum value at 160 °C. According to the above research, increasing temperature can accelerate the diffusion of nonpolar components and improve the binding energy. However, due to the presence of silica particles, the diffusion rate of the saturate component is greatly affected at high temperature, and the aromatic component plays a dominant role in diffusion. Therefore, in order to improve the diffusion capacity, it is recommended to choose a regenerator rich in the aromatic component, which can fully realize the performance recovery of aged asphalt.

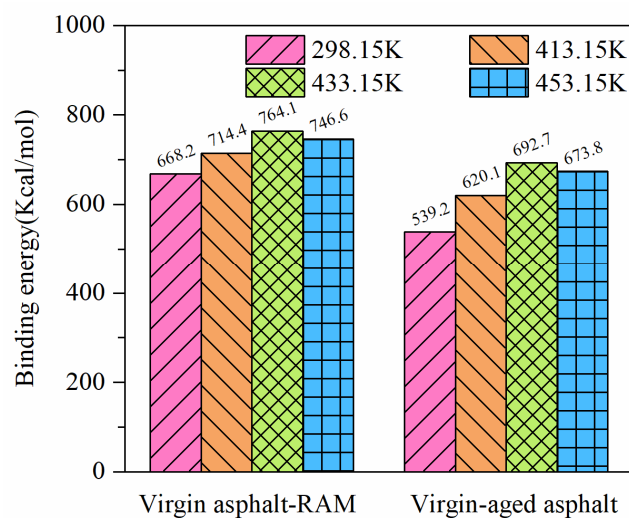


**Figure 16.** Binding energies of virgin–aged asphalt and virgin asphalt–RAM at different temperatures.

### 3.3.2. Mutual Diffusion Coefficient

The diffusion behavior for virgin asphalt–RAM is one of the key points to determine whether a homogeneous recycled asphalt can be achieved. The difference in concentration between the two regions will cause mutual diffusion at the molecular level. If the concentrations are equal, the interdiffusion process ceases. Figure 17 shows the evolution of molecules for virgin asphalt–RAM at 433 K during the mutual diffusion. As shown in Figure 17, the snapshots of the model (virgin asphalt–RAM) at the simulation times of 125, 250, 375 and 500 ps are extracted. Virgin asphalt is concentrated on the left side of the simulation box, and the RAM is on the other side. To sufficiently exhibit diffusion processes of virgin asphalt, the molecules of RAM are set to be invisible in sequence. It can be clearly observed that SARA components continuously move across the border and penetrate into RAM with time. It is discovered that SARA components gradually penetrate into the area of RAM. Furthermore, the penetration depth and number of asphaltene molecules in RAM are obviously less than those of the other three components, indicating the lower diffusion capacity.

The above phenomenon can well represent the mutual diffusion process of the model, but it cannot quantify the diffusion rate. As shown in Figure 18, the relative concentration of virgin asphalt along the  $z$  direction is monitored during the simulation processes. It can be found that the curves of relative concentration have similar shapes even at different simulation temperatures. The relative concentration of virgin asphalt reduces at higher  $z$  positions as the temperature increases while it rises at lower  $z$  positions, which illustrated the diffusive phenomena of virgin asphalt into RAM, and diffusion processes favorably followed Fick's second law of diffusion. Under different simulation time steps, the penetration depth can be obtained.

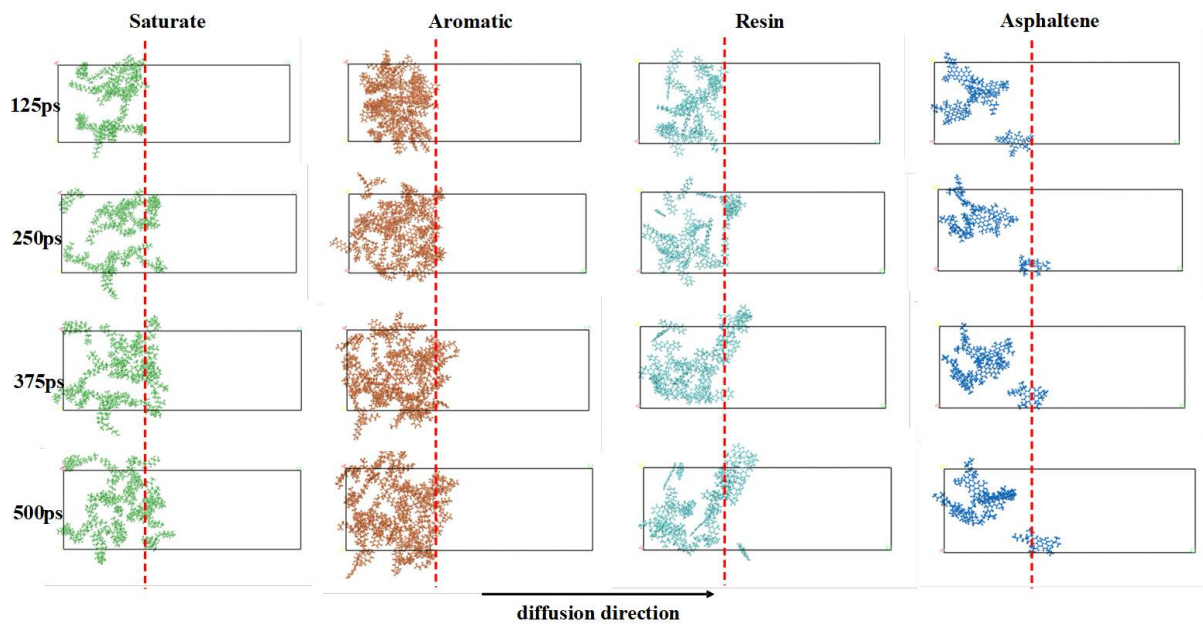


Figure 17. Diffusion process (virgin asphalt–RAM).

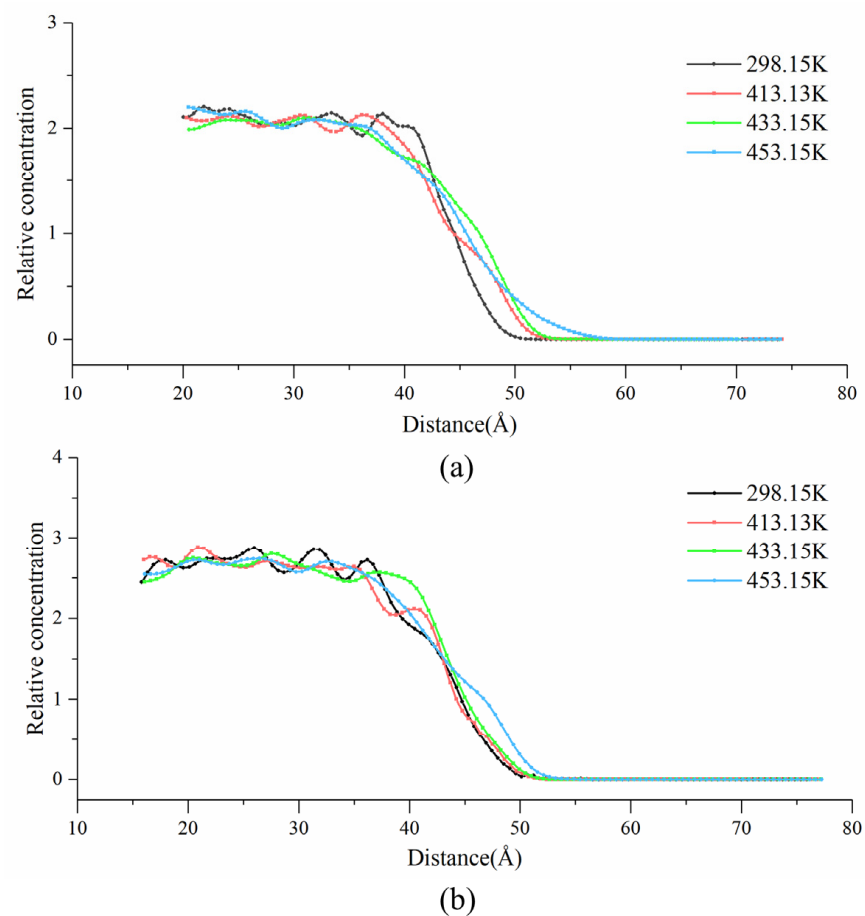


Figure 18. Evolution curves of relative concentration of virgin asphalt with simulation temperature in virgin-aged asphalt and virgin asphalt–RAM: (a) virgin-aged asphalt; (b) virgin asphalt–RAM.

Fick's second law describes the variability of molecule concentration and diffusion length with time, as shown in Equation (7).

$$\frac{\partial c}{\partial t} = \frac{\partial}{\partial z} \left( D(c) \frac{\partial c}{\partial z} \right) \quad (7)$$

where  $t$  refers to time;  $z$  refers to the length along the diffusion direction;  $c$  is the concentration; and  $D(c)$  is the diffusivity dependent on the concentration.

Assuming  $D(c) = D_0$  is a constant, the equation has a simple solution as shown in Equation (8). In this study, this assumption is adopted and the equation is applied to calculate the interdiffusion coefficient of virgin asphalt into RAM,

$$c(z, t) = c_0 \left( 1 - \operatorname{erf} \left( \frac{z}{2\sqrt{D_0 t}} \right) \right) \quad (8)$$

where  $c(z, t)$  refers to the function of concentration which depends on time and length along the direction;  $\operatorname{erf}()$  is the error function;  $D_0$  is the diffusion coefficient; and  $c_0$  is the fitted concentration value.

Using Equation (8) to fit the extracted data from the relative concentration in the MD simulation, the length of diffusion region and diffusion coefficients of virgin asphalt–RAM are obtained and presented in Tables 3 and 4. A larger diffusion coefficient means a faster diffusion rate.

**Table 3.** Diffusion region length of virgin asphalt–RAM.

$z$ (Å)	413.15 K	433.15 K	453.15 K
Virgin-aged asphalt	51.36	54.28	57.04
Virgin asphalt–RAM	51.07	53.92	56.99

**Table 4.** Diffusion coefficients of virgin asphalt–RAM.

$D_0$ (m <sup>2</sup> /s)	413.15 K	433.15 K	453.15 K
Virgin-aged asphalt	$1.012 \times 10^{-9}$	$1.167 \times 10^{-9}$	$1.254 \times 10^{-9}$
Virgin asphalt–RAM	$1.006 \times 10^{-9}$	$1.126 \times 10^{-9}$	$1.202 \times 10^{-9}$

Temperature makes a great difference to the diffusion performance of asphalt, but the effect of temperature on the dominant force has not been fully revealed in the process of mutual diffusion. For the above problem, the diffusion state at 413.15 K, 433.15 K and 453.15 K is explored. The results of diffusion region length and interdiffusion coefficients of virgin-aged asphalt and virgin asphalt–RAM at three temperatures are presented in Tables 3 and 4, respectively. Diffusion coefficients of virgin asphalt–RAM are always lower than that of virgin-aged asphalt, indicating that the presence of silica particles inhibits diffusion behaviors, which is in great agreement with the research findings. It can be concluded from Table 4 that the interdiffusion coefficient grows as temperature increases. When the temperature increases from 413.15 K to 453.15 K, the interdiffusion coefficient of virgin-aged asphalt increases by 29.7–93.6%, while that of virgin asphalt–RAM only increases by 32.3–57.3%. Diffusion coefficients of virgin-aged asphalt have more significant changes than that of virgin asphalt–RAM, which means that diffusion behaviors of virgin-aged asphalt are more susceptible to the temperature. If the temperature is increased, the diffusion capacity of virgin asphalt–RAM is closest to that of virgin-aged asphalt at 433.15 K. In addition, when the temperature rises to 453.15 K, the diffusion capacity increases little, and may lead to asphalt aging. Above all, silica particles have great influence on saturated phenol at high temperature, which is not conducive to diffusion. Therefore, it is recommended to raise the temperature appropriately during construction, but control it at about 433.15–453.15 K.

#### 4. Conclusions

In this study, diffusion behaviors and blending efficiencies of virgin asphalt–RAM are explored based on the MD simulation. The conclusions are drawn from the analysis as the following:

(1) The mutual diffusion model of virgin asphalt–RAM is established and verified by different thermodynamic properties of virgin asphalt and aged asphalt.

(2) The presence of silica particles does not change the diffusion direction, and the diffusion behavior of virgin asphalt–RAM gradually moving towards each other is dominated by the migration of virgin asphalt. As the temperature increases, the diffusion efficiency is improved, and the effect of diffusion efficiency on virgin–aged asphalt is more significant than that of virgin asphalt–RAM.

(3) In the diffusion process, the polar components have obvious self-aggregation behaviors and gradually form a more compact colloidal structure under the influence of silica particles, which also promotes the formation of a barrier by asphaltene and resin to prevent the diffusion of molecules.

(4) The SARA components struggle to separate and fully achieve mutual diffusion in the diffusion processes, which is on account of the low energy between virgin asphalt and RAM.

(5) The presence of silica particles significantly slows down the diffusion rate. In order to promote blending efficiency of virgin asphalt–RAM, it is suggested that a regenerator with enough aromatic components should be added or the temperature should be raised within the allowable range and controlled at about 433.15–453.15 K.

**Author Contributions:** Conceptualization and funding acquisition, X.Q. and Q.Y.; methodology, S.X.; software, K.L.; data curation, W.X.; formal analysis and writing—original draft preparation, S.C.; writing—review and editing, Q.Y., X.Q., K.L., S.X. and W.X. All authors have read and agreed to the published version of the manuscript.

**Funding:** This study was funded by Natural Science Foundation of Zhejiang Province, grant number LY23E080002 and LY21E080011, and Science and Technology Plan Project of Jinhua Technology Bureau, grant number 2021-3-175 and 2022-3-072.

**Data Availability Statement:** The data presented in this study are available on request from the corresponding author.

**Acknowledgments:** The authors are great grateful for the assistance from Ke Yang and Xin Wang in conducting experiments for this paper. The authors would like to thank Jingxian Xu and Ganghua Hu for commendable opinions and revising the English style of the manuscript, which improved its legibility.

**Conflicts of Interest:** The authors declare that they have no known competing financial interest or personal relationship that could have appeared to influence the work reported in this paper.

#### References

1. Gao, J.; Yao, Y.; Yang, J.; Song, L.; Xu, J.; He, L.; Tao, W. Migration behavior of reclaimed asphalt pavement mastic during hot mixing. *J. Clean. Prod.* **2022**, *376*, 134123. [[CrossRef](#)]
2. Jiang, Y.; Gu, X.; Zhou, Z.; Ni, F.; Dong, Q. Laboratory Observation and Evaluation of Asphalt Blends of Reclaimed Asphalt Pavement Binder with Virgin Binder using SEM/EDS. *Transp. Res. Rec. J. Transp. Res. Board* **2018**, *2672*, 69–78. [[CrossRef](#)]
3. Li, N.; Tang, W.; Yu, X.; Zhan, H.; Wang, X.; Wang, Z. Laboratory investigation on blending process of reclaimed asphalt mixture. *Constr. Build. Mater.* **2022**, *325*, 126793. [[CrossRef](#)]
4. Nahar, S.N.; Mohajeri, M.; Schmets, A.J.M.; Scarpas, A.; van de Ven, M.F.C.; Schitter, G. First Observation of Blending-Zone Morphology at Interface of Reclaimed Asphalt Binder and Virgin Bitumen. *Transp. Res. Rec. J. Transp. Res. Board* **2013**, *2370*, 1–9. [[CrossRef](#)]
5. Zhao, S.; Nahar, S.N.; Schmets, A.J.; Huang, B.; Shu, X.; Scarpas, T. Investigation on the microstructure of recycled asphalt shingle binder and its blending with virgin bitumen. *Road Mater. Pavement Des.* **2015**, *16* (Suppl. 1), 21–38. [[CrossRef](#)]
6. Li, L.B. Study on non-fickian diffusion in glassy polymer. *Chin. J. Biomed. Eng.* **1999**, *18*, 441–450.
7. Zhang, Y.X.; Ling, T.Q. Micro mechanism between recycling agent and aged asphalt. *J. Civ. Archit. Environ. Eng.* **2010**, *32*, 55–59.

8. Ding, L.L.; Huang, X.M. Diffusion mechanism of asphalt rejuvenation agent and research on diffusion simulation test. *Transp. Sci. Technol.* **2009**, *5*, 75–78.
9. Ma, T.; Huang, X.; Zhang, J. Recycling law of aged asphalt based on composite theory of material. *J. Southeast Univ. Nat. Sci. Ed.* **2008**, *38*, 520–524.
10. Tao, X.H. Research on mechanism of asphalt film transfer based on convective mass transfer theory. *J. Highw. Transp. Dev.* **2010**, *27*, 21–24.
11. Tang, B.M.; Ding, Y.J.; Zhu, H.Z.; Cao, X.J. Study on Agglomeration Variation Pattern of Asphalt Molecules. *China J. Highw. Transp.* **2013**, *26*, 50.
12. Rathore, M.; Haritonovs, V.; Meri, R.M.; Zaumanis, M. Rheological and chemical evaluation of aging in 100% reclaimed asphalt mixtures containing rejuvenators. *Constr. Build. Mater.* **2022**, *318*, 126026. [[CrossRef](#)]
13. Chen, L.; He, Z.Y.; Chen, H.B.; Wang, X.D.; Xiang, H. Rheological Characteristics and MDs Simulation of Interface Regeneration Between Virgin and Aged Asphalts. *China J. Highw. Transp.* **2019**, *32*, 25–33.
14. Ding, Y.; Deng, M.; Cao, X.; Yu, M.; Tang, B. Investigation of mixing effect and molecular aggregation between virgin and aged asphalt. *Constr. Build. Mater.* **2019**, *221*, 301–307. [[CrossRef](#)]
15. Vassaux, S.; Gaudefroy, V.; Boulangé, L.; Soro, L.J.; Pévère, A.; Michelet, A.; Mouillet, V. Study of remobilization phenomena at reclaimed asphalt binder/virgin binder interphases for recycled asphalt mixtures using novel microscopic methodologies. *Constr. Build. Mater.* **2018**, *165*, 846–858. [[CrossRef](#)]
16. Hettiarachchi, C.; Hou, X.; Xiang, Q.; Yong, D.; Xiao, F. A blending efficiency model for virgin and aged binders in recycled asphalt mixtures based on blending temperature and duration. *Resour. Conserv. Recycl.* **2020**, *161*, 104957. [[CrossRef](#)]
17. Yang, C.; Zhang, J.; Yang, F.; Cheng, M.; Wang, Y.; Amirhanian, S.; Wu, S.; Wei, M.; Xie, J. Multi-scale performance evaluation and correlation analysis of blended asphalt and recycled asphalt mixtures incorporating high RAP content. *J. Clean. Prod.* **2021**, *317*, 128278. [[CrossRef](#)]
18. Wu, J.; Liu, Q.; Yang, S.; Oeser, M.; Ago, C. Study of migration and diffusion during the mixing process of asphalt mixtures with RAP. *Road Mater. Pavement Des.* **2020**, *22*, 1578–1593. [[CrossRef](#)]
19. Ding, Y.; Huang, B.; Shu, X. Blending efficiency evaluation of plant asphalt mixtures using fluorescence microscopy. *Constr. Build. Mater.* **2018**, *161*, 461–467. [[CrossRef](#)]
20. Chen, L.; Chen, H.B.; Li, P. Quantitative Evaluation on Interfacial Diffusion Behavior of Asphalt with High Percentage of RAP. *J. Build. Mater.* **2021**, *4*, 811–819.
21. Pape, S.E.; Castorena, C.A. Assessment of the impacts of sample preparation on the use of EDS for analyzing recycled asphalt blending. *J. Microsc.* **2021**, *283*, 232–242. [[CrossRef](#)]
22. Ding, L.; Wang, X.; Zhang, M.; Chen, Z.; Meng, J.; Shao, X. Morphology and properties changes of virgin and aged asphalt after fusion. *Constr. Build. Mater.* **2021**, *291*, 123284. [[CrossRef](#)]
23. Roja, K.L.; Masad, E.; Vajipeyajula, B.; Yiming, W.; Khalid, E.; Shunmugasamy, V.C. Chemical and multi-scale material properties of recycled and blended asphalt binders. *Constr. Build. Mater.* **2020**, *261*, 119689. [[CrossRef](#)]
24. Zhan, Y.; Wu, H.; Song, W.; Zhu, L. MDs Study of the Diffusion between Virgin and Aged Asphalt Binder. *Coatings* **2022**, *12*, 403. [[CrossRef](#)]
25. Huang, M.; Zhang, H.; Gao, Y.; Wang, L. Study of diffusion characteristics of asphalt–aggregate interface with MDs simulation. *Int. J. Pavement Eng.* **2019**, *22*, 319–330. [[CrossRef](#)]
26. Xu, M.; Yi, J.; Feng, D.; Huang, Y. Diffusion characteristics of asphalt rejuvenators based on MDs simulation. *Int. J. Pavement Eng.* **2017**, *20*, 615–627. [[CrossRef](#)]
27. Xu, G.; Wang, H.; Sun, W. MDs study of rejuvenator effect on RAP binder: Diffusion behavior and molecular structure. *Constr. Build. Mater.* **2018**, *158*, 1046–1054. [[CrossRef](#)]
28. Sun, W.; Wang, H. MDs simulation of diffusion coefficients between different types of rejuvenator and aged asphalt binder. *Int. J. Pavement Eng.* **2020**, *21*, 966–976. [[CrossRef](#)]
29. Li, D.D.; Greenfield, M.L. Chemical compositions of improved model asphalt systems for molecular simulations. *Fuel* **2014**, *115*, 347–356. [[CrossRef](#)]
30. Qu, X.; Liu, Q.; Guo, M.; Wang, D.; Oeser, M. Study on the effect of aging on physical properties of asphalt binder from a microscale perspective. *Constr. Build. Mater.* **2018**, *187*, 718–729. [[CrossRef](#)]
31. Cui, B.; Gu, X.; Wang, H. Numerical and experimental evaluation of adhesion properties of asphalt–aggregate interfaces using MDs simulation and atomic force microscopy. *Road Mater. Pavement Des.* **2022**, *23*, 1564–1584. [[CrossRef](#)]
32. Cui, B.Y. *The Blending Mechanism of Virgin and Aged Asphalt Binders in Hot Recycled Asphalt Based on MDs Simulations*; Southeast University: Nanjing, China, 2020.
33. Zhu, X.; Du, Z.; Ling, H.; Chen, L.; Wang, Y. Effect of filler on thermodynamic and mechanical behaviour of asphalt mastic: A MD simulation study. *Int. J. Pavement Eng.* **2018**, *21*, 1248–1262. [[CrossRef](#)]
34. Zhang, J.P.; Pei, J.Z.; Li, Y.W. Research on Interaction between Asphalt and Filler Based on DSR Test. *Adv. Mater. Res.* **2013**, *723*, 480–487. [[CrossRef](#)]
35. Long, Z.; You, L.; Tang, X.; Ma, W.; Ding, Y.; Xu, F. Analysis of interfacial adhesion properties of nano-silica modified asphalt mixtures using MDs simulation. *Constr. Build. Mater.* **2020**, *255*, 119354. [[CrossRef](#)]

36. Khabaz, F.; Khare, R. Glass Transition and Molecular Mobility in Styrene-Butadiene Rubber Modified Asphalt. *J. Phys. Chem. B* **2015**, *119*, 14261–14269. [[CrossRef](#)] [[PubMed](#)]
37. Gao, Y.; Zhang, Y.; Yang, Y.; Zhang, J.H.; Gu, F. MDs investigation of interfacial adhesion between oxidised bitumen and mineral surfaces. *Appl. Surf. Sci.* **2019**, *479*, 449–462. [[CrossRef](#)]
38. Xu, G.; Wang, H. MDs study of oxidative aging effect on asphalt binder properties. *Fuel* **2017**, *188*, 1–10. [[CrossRef](#)]
39. Wang, P.; Dong, Z.-J.; Tan, Y.-Q.; Liu, Z.-Y. Investigating the Interactions of the Saturate, Aromatic, Resin, and Asphaltene Four Fractions in Asphalt Binders by Molecular Simulations. *Energy Fuels* **2015**, *29*, 112–121. [[CrossRef](#)]
40. Ding, Y.; Huang, B.; Shu, X.; Zhang, Y.Z.; Woods, M.E. Use of MDs to investigate diffusion between virgin and aged asphalt binders. *Fuel* **2016**, *174*, 267–273. [[CrossRef](#)]
41. Liu, J.; Liu, Q.; Wang, S.; Zhang, X.Y.; Xiao, C.Y.; Yu, B. MDs evaluation of activation mechanism of rejuvenator in reclaimed asphalt pavement (RAP) binder. *Constr. Build. Mater.* **2021**, *298*, 123898. [[CrossRef](#)]

**Disclaimer/Publisher’s Note:** The statements, opinions and data contained in all publications are solely those of the individual author(s) and contributor(s) and not of MDPI and/or the editor(s). MDPI and/or the editor(s) disclaim responsibility for any injury to people or property resulting from any ideas, methods, instructions or products referred to in the content.